

# Hybridized Electromagnetic—Trieboelectric Nanogenerator for Scavenging Air-Flow Energy to Sustainably Power Temperature Sensors

Xue Wang,<sup>†</sup> Shuhua Wang,<sup>†</sup> Ya Yang,<sup>\*,†</sup> and Zhong Lin Wang<sup>\*,†,||</sup>

<sup>†</sup>Beijing Institute of Nanoenergy and Nanosystems, Chinese Academy of Sciences, Beijing 100083, China and <sup>||</sup>School of Materials Science and Engineering, Georgia Institute of Technology, Atlanta, Georgia 30332-0245, United States

**ABSTRACT** We report a hybridized nanogenerator with dimensions of 6.7 cm × 4.5 cm × 2 cm and a weight of 42.3 g that consists of two triboelectric nanogenerators (TENGs) and two electromagnetic generators (EMGs) for scavenging air-flow energy. Under an air-flow speed of about 18 m/s, the hybridized nanogenerator can deliver largest output powers of 3.5 mW for one TENG (in correspondence of power per unit mass/volume: 8.8 mW/g and 14.6 kW/m<sup>3</sup>) at a loading resistance of 3 MΩ and 1.8 mW for one EMG (in correspondence of power per unit mass/volume: 0.3 mW/g and 0.4 kW/m<sup>3</sup>) at a loading resistance of 2 kΩ, respectively. The hybridized nanogenerator can be utilized to charge a capacitor of 3300 μF to sustainably power four temperature sensors for realizing self-powered temperature sensor networks. Moreover, a wireless temperature sensor driven by a hybridized nanogenerator charged Li-ion battery can work well to send the temperature data to a receiver/computer at a distance of 1.5 m. This work takes a significant step toward air-flow energy harvesting and its potential applications in self-powered wireless sensor networks.



**KEYWORDS:** hybridized nanogenerator · triboelectric nanogenerator · electromagnetic generator · self-powered sensor · wind energy · air-flow energy

As mobile electronic devices and wireless sensors rapidly increase, small-size energy harvesters have attracted considerable interest due to their capability of replacing the conventional Li-ion battery to realize self-powered devices and systems.<sup>1–3</sup> As one of the most important renewable energy sources in nature, air-flow/wind energy has attracted special interest due to its abundance, ubiquity, and large energy capacity.<sup>4,5</sup> On the basis of the electromagnetic effect, the electromagnetic wind turbine as the most widely used type of air-flow energy harvester has been extensively developed.<sup>6</sup> The main drawbacks of this air-flow energy harvester are the complex structure and the large volume, which have retarded the process of down-scaling. In order to implement the air-flow energy harvester on mobile devices or sensors, it is necessary to develop new design strategies and techniques to realize both miniaturized devices and high performance.

By utilizing a combined mechanism of contact electrification and electrostatic induction, triboelectric nanogenerators (TENGs) have been widely utilized to effectively scavenge mechanical energy.<sup>7–10</sup> The reported TENGs exhibit obvious characteristics of simple structure, low cost, light weight, and high power density. By utilizing an air-flow induced vibration of an organic film in an acrylic tube to realize the periodic contact/separation between two triboelectric materials with different triboelectric polarities, some attempts to use TENGs for scavenging air-flow energy to light up light-emitting diodes (LEDs) have been demonstrated.<sup>11–14</sup> Moreover, the optimized output performance of TENG has been achieved by modulating the device sizes and electrode gaps.<sup>15</sup> However, the obtained electric power is still not high enough to sustainably power some mobile electronic devices or sensors with larger power demand. The air-flow induced vibration of the film only has the contributions to the output of the TENG at

\* Address correspondence to yayang@binn.cas.cn, zlwang@gatech.edu.

Received for review February 21, 2015 and accepted April 6, 2015.

Published online 10.1021/acs.nano.5b01187

© XXXX American Chemical Society

the free-standing end of the film, where the produced vibration energy at the front section of the film was wasted since this section cannot contact the triboelectric materials at the top and bottom of the acrylic tube as governed by the working principle of TENG. Harvesting the wasted vibration energy in this kind of device could enhance the total output performance of the device further, which is challenging owing to the lack of techniques.

A hybridized mechanical energy scavenging technology may be utilized to solve this issue by integrating TENGs and the electromagnetic generators (EMGs).<sup>16–18</sup> More electricity can be obtained from the same mechanical motions by using this technique, which may achieve the self-powered mobile devices or sensors. The difficulty is how to realize the simultaneous working of the two energy harvesting units to produce enough energy. In this paper, we demonstrated a hybridized electromagnetic-triboelectric nanogenerator to convert the kinetic energy of the air-flow into electric energy for sustainably powering temperature sensors. The air-flow-driven vibration of a kapton film in an acrylic tube can induce the simultaneous working of two TENGs at the free-standing end and two electromagnetic generators (EMGs) at the front section of the device. The fabricated device has small dimensions of 6.7 cm × 4.5 cm × 2 cm and the lightweight of 42.3 g, which can be directly integrated with commercial temperature sensors. The hybridized nanogenerator has much better charging performance than that of individual energy harvesting unit (TENG or EMG). Four temperature sensors have been sustainably powered by utilizing the hybridized nanogenerator without using a Li-ion battery. The produced electric energy can be also stored in a Li-ion battery for driving a wireless temperature sensor or other uses.

## RESULTS AND DISCUSSION

As shown in Figure 1a,b, the schematic diagram of the hybridized nanogenerator displays the detailed structures of the device, where the TENG is composed of a polytetrafluoroethylene (PTFE) film coated with a Cu electrode and another Cu electrode on the kapton film. The EMG consists of a planar coil and a magnet fixed on the kapton film. When the wind flows into the acrylic tube, the vibration behavior of the kapton can result in the working of both TENG and EMG. Parts c and d of Figure 1 are photographs of the fabricated device, showing that the hybridized nanogenerator has small inner dimensions of 6.7 cm × 4 cm × 1.2 cm. Figure 1e presents sequential images of the contact and separation process for the kapton film in the acrylic tube in one cycle under an air-flow speed of about 18 m/s, which was captured by using a high-speed camera at a frame rate of 7500 Hz. The dynamic process for the air-flow driven vibration behavior of the kapton

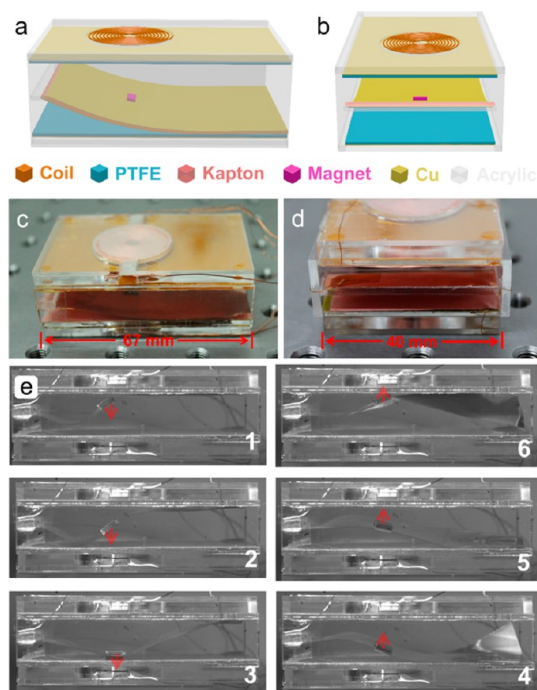


**Figure 1.** (a, b) Schematic diagrams of the hybridized electromagnetic-triboelectric nanogenerator. (c, d) Photographs of the fabricated hybridized nanogenerator. (e) Photographs of the device under the different vibrations of the kapton film in the acrylic tube captured by using a high speed camera.

film can be also seen in the movie file-1 in Supporting Information.

Figure 2 displays the electricity generation process of two TENGs and two EMGs in one cycle, where the deformations of the kapton film are confirmed by using the photographs in Figure 1e. For the status-1, a portion of the top PTFE film and a portion of the Cu film on the kapton film are brought into fully contact with each other, which can generate the triboelectric charges due to the different triboelectric polarities. According to the triboelectric series, PTFE is much more triboelectrically negative than Cu, indicating the positive and negative triboelectric charges occur on the surfaces of Cu and PTFE, respectively. The produced triboelectric charges on the PTFE film can be preserved on the surface for a long time due to the nature of the insulator.<sup>19</sup> There is no electrical output for both the TENG and EMG. For the status-2, the magnets on the kapton film moved down, which can induce the separation between the top PTFE film and the Cu electrode on the kapton film. Because of the electrostatic induction, the inner electric field can drive the electrons to flow from the top Cu electrode on the PTFE film to the Cu electrode on the kapton film, resulting in an observed current/voltage signal for the TENG-1. Moreover, when the magnets were moved down from status-1 to status-2, the magnetic flux in both top and bottom coils could be changed, resulting in the flow of current in the coils due to Lorentz force. When the magnets were moved down, the magnetic

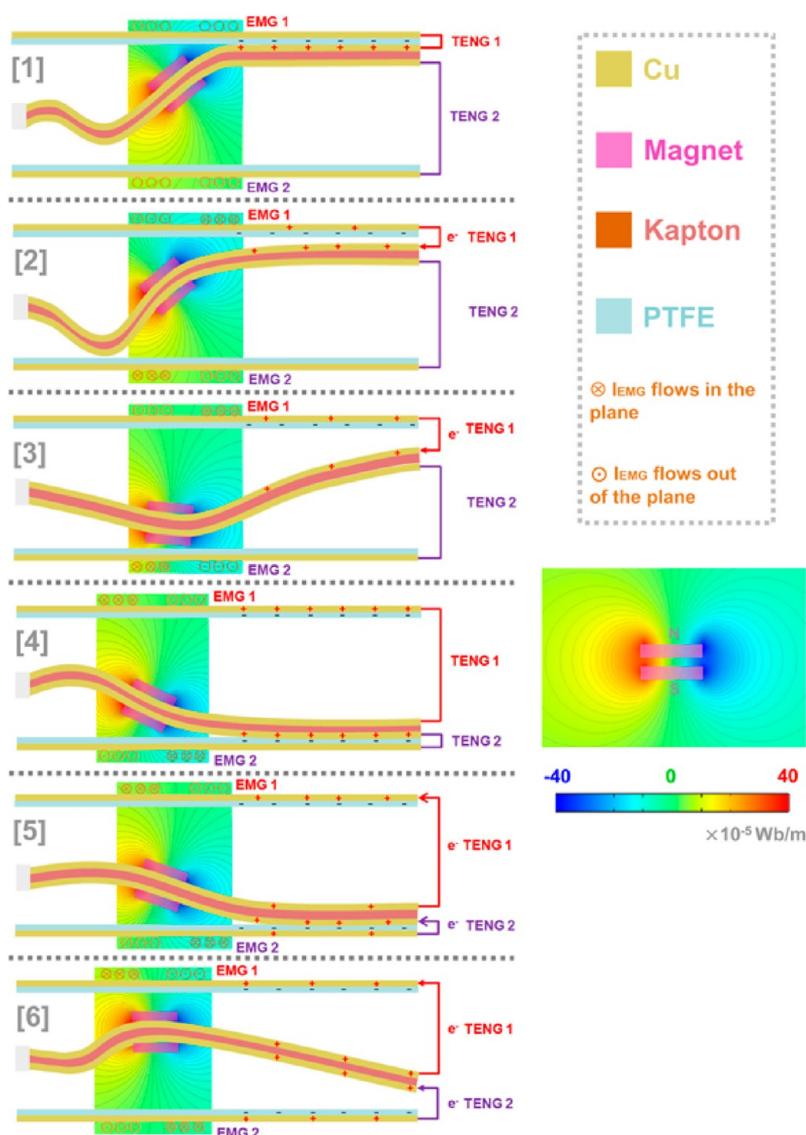


Figure 2. Schematic diagrams of the operating principle for the hybridized electromagnetic-triboelectric nanogenerator.

flux through the top and bottom coils could decrease and increase, respectively, indicating the opposite current signals occur in the top and bottom coils. The output current/voltage of the two EMGs lasted when the magnets were moved down and up in the acrylic tube. For the TENGs, when the Cu electrode on the kapton film was moved to contact the bottom PTFE, the triboelectric charges were created on the Cu and PTFE (status-4). The output current/voltage signals of both TENG-1 and TENG-2 were observed when the kapton film was moved back from bottom to top. Both the TENGs and EMGs deliver the alternating current (AC) signals in the external circuit.

Under an air-flow speed of 18 m/s, the short-circuit current ( $I_{sc}$ ) of TENG 1 is  $55.7 \pm 8.1 \mu\text{A}$  (Figure 3a), where the statistic data include the maximum peak values of 50% or more (Figure S1, Supporting Information). Figure 3b illustrates the resistance dependence of both output current and power of the TENG 1 with the loading

resistances ranged from  $10^3 \Omega$  to  $10^9 \Omega$ . The output current of TENG-1 decreases with increasing the loading resistance, while the output power increases in the resistance region from  $10^3 \Omega$  to  $3 \text{ M}\Omega$  and then decreases under the larger loading resistances ( $>3 \text{ M}\Omega$ ). The largest output power of TENG 1 reaches 3.5 mW (in correspondence of power per unit mass/volume:  $8.8 \text{ mW/g}$  and  $14.6 \text{ kW/m}^3$ ) at a loading resistance of  $3 \text{ M}\Omega$ , where the calculation of the power density includes a half of the total mass and volume for two TENGs. Figure 3c indicates that the  $I_{sc}$  of the TENG 2 is  $52.7 \pm 8.6 \mu\text{A}$  (Figure S2, Supporting Information), where the output current of the device decreases with increasing the loading resistance, as depicted in Figure 3d. The largest output power of TENG 2 is about 3.3 mW (in correspondence of power per unit mass/volume:  $8.3 \text{ mW/g}$  and  $13.8 \text{ kW/m}^3$ ) at the loading resistance of  $3 \text{ M}\Omega$ .

To demonstrate that the produced energy can be stored, Figure 3e illustrates the charging curves of the

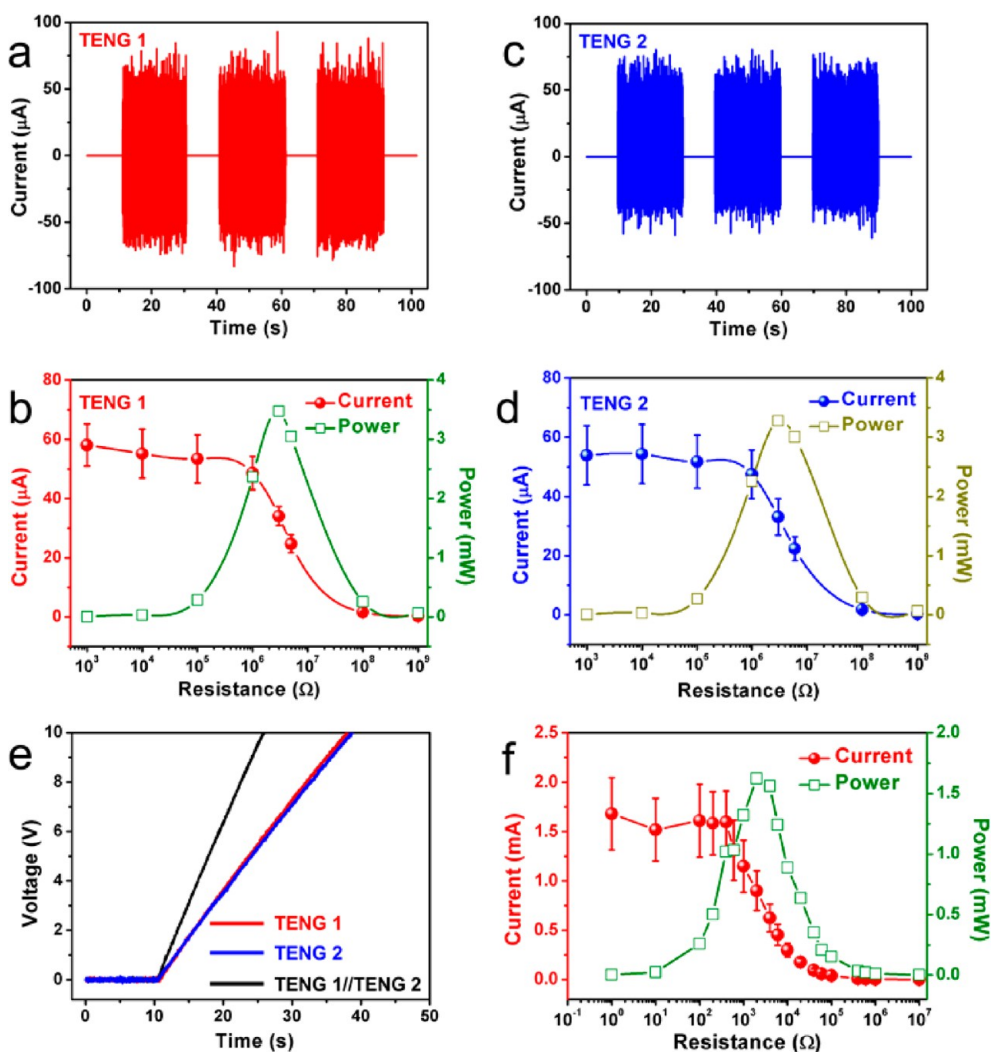


Figure 3. (a, c) Short-circuit current signals of TENG 1 (a) and TENG 2 (c). (b, d) Output current and power of TENG 1 (b) and TENG 2 (d) under the different loading resistances. (e) Measured charging voltage curves of a capacitor with  $10 \mu\text{F}$  by using the different devices. (f) Output current and power of TENG 1 after using a transformer.

TENG 1, TENG 2, and TENG 1//TENG 2 units for charging a capacitor of  $10 \mu\text{F}$ , where the rectification circuits were used for devices. It can be seen that the two TENGs have similar charging performances, and the integrated device (TENG 1//TENG 2) has a much better charging performance than that of the individual energy harvesting unit (TENG 1 or TENG 2). Since the TENGs have the high output impedance of  $3 \text{ M}\Omega$ , it is necessary to use a transformer to decrease the impedance and increase the output current. As shown in Figure 3f, the output current of the TENG 1 after using a transformer decreases with increasing the loading resistance (Figures S3 and S4, Supporting Information), where the  $I_{\text{sc}}$  of device is about  $2.2 \text{ mA}$  and the largest output power is about  $1.8 \text{ mW}$  at a loading resistance of  $2 \text{ k}\Omega$ .

Parts a and b of Figure 4 show the  $I_{\text{sc}}$  and open-circuit voltage ( $V_{\text{oc}}$ ) of the EMG 1, respectively. The corresponding current and voltage are about  $1.6 \pm 0.3 \text{ mA}$  and  $2.4 \pm 0.5 \text{ V}$ , respectively. As depicted in Figure 4c, the output current of EMG 1 decreases with

increasing the loading resistance (Figure S5, Supporting Information), and the largest output power is about  $1 \text{ mW}$  (in correspondence of power per unit mass/volume:  $0.2 \text{ mW/g}$  and  $0.2 \text{ kW/m}^3$ ) at the loading resistance of  $2 \text{ k}\Omega$ . As illustrated in Figure 4d,e, the  $I_{\text{sc}}$  and  $V_{\text{oc}}$  of EMG 2 are about  $2.3 \pm 0.3 \text{ mA}$  and  $3.3 \pm 0.4 \text{ V}$ , respectively. Figure 4f shows that the output current of EMG 2 increases with increasing the loading resistances (Figure S6, Supporting Information), and the largest output power of the device is about  $1.8 \text{ mW}$  (in correspondence of power per unit mass/volume:  $0.3 \text{ mW/g}$  and  $0.4 \text{ kW/m}^3$ ) at the loading resistance of  $2 \text{ k}\Omega$ .

To compare the output performances of the TENGs and EMGs, the generated electric energy  $E_{\text{electricity}}$  for each energy harvesting unit has been calculated, where the  $E_{\text{electricity}}$  can be given by

$$E_{\text{electricity}} = \int_{t_1}^{t_2} I^2 R dt \quad (1)$$

where  $I$  is the output current of the device,  $R$  is the loading resistance, and  $t$  is the time. Under the time

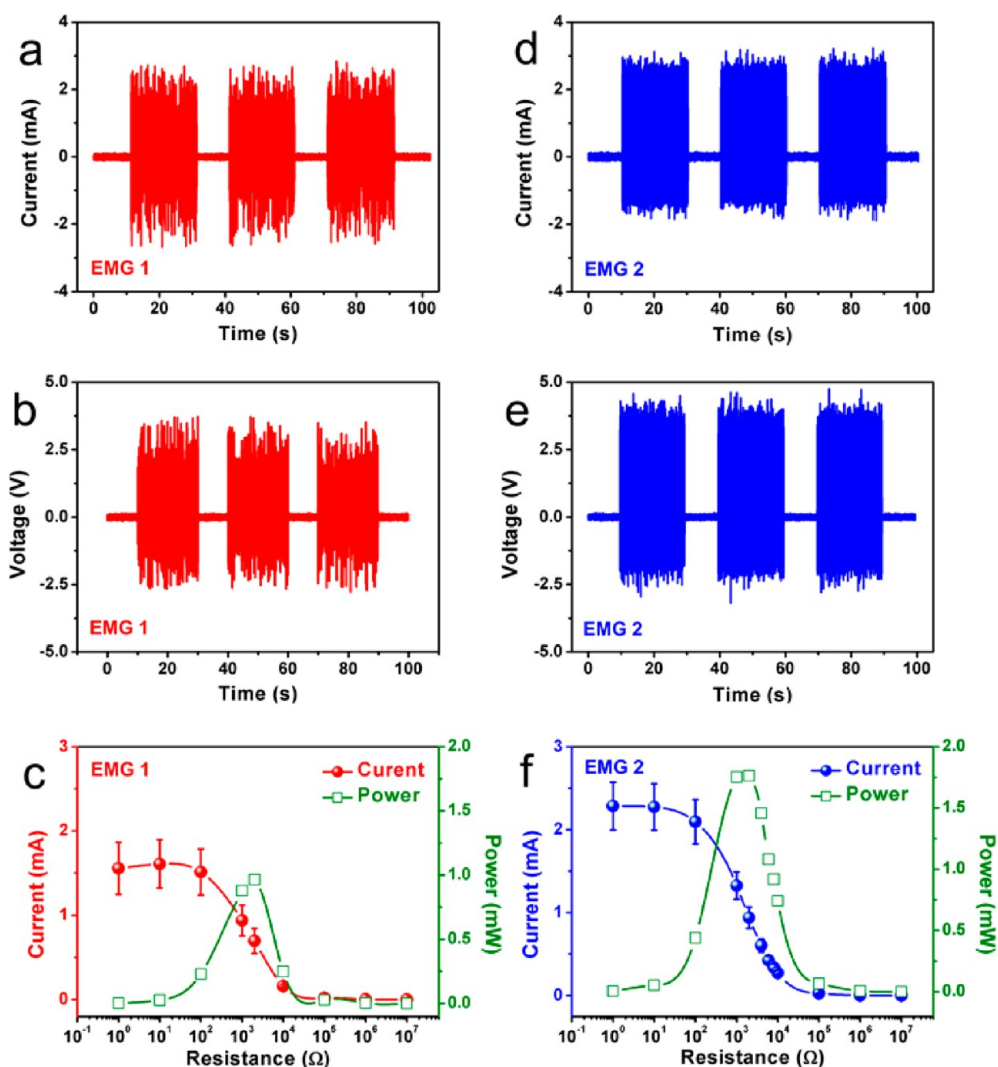


Figure 4. (a, b) Short-circuit current (a) and open-circuit voltage (b) of EMG 1. (c) Output current and power of EMG 1 under the different loading resistances. (d, e) Short-circuit current (d) and open-circuit voltage (e) of EMG 2. (f) Output current and power of EMG 2 under the different loading resistances.

interval between  $t_1$  and  $t_2$  (10 s), parts a and b of Figure 5 show that the produced electrical energies of TENG 1 and TENG 2 are about 1.4 and 1.2 mJ, respectively, so that the total electric energy is 2.6 mJ for two TENGs. As depicted in Figure 5c,d, the produced electrical energies of EMG 1 and EMG 2 are about 0.7 and 2.5 mJ, respectively, so that the total electrical energy of the two EMGs is 3.2 mJ in 10 s. As a result, the hybridized nanogenerator can produce a total electrical energy of 5.8 mJ in 10 s, which is much larger than that produced by a single energy harvesting unit (TENG or EMG). The difference for the output performances of two TENGs is associated with the different contact/separation conditions between the Cu film on kapton film and the top or bottom PTFE film. Moreover, the similar difference for the output performances of two EMGs is also due to the difference of dynamic processes for the vibration of kapton film, which can be clearly seen in the movie file-1 (Supporting Information).

To demonstrate that the hybridized nanogenerator can be used as a mobile power source to power some electronic devices, the TENG and the EMG were connected to two groups of LEDs, as shown in Figure 5e. Figure 5f shows that these LEDs can be directly lighted up by the air-flow driven hybridized nanogenerator (movie file-2, Supporting Information). Moreover, these LEDs driven by the hybridized nanogenerator can provide enough illumination for reading printed text in complete darkness, as displayed in Figure 5g,h (movie file-3, Supporting Information). As illustrated in Figure 5i,j, the corresponding illumination intensities of the two groups of LEDs are larger than 10 lx.

To realize that the hybridized nanogenerator can be used to sustainably power temperature sensors, it is necessary to store the produced energy in a capacitor first. Figure 6a presents the rectified output current signals of the TENG with transformer, EMG, and the hybridized device (EMG/TENG with transformer), showing that no obvious enhancement effect can be

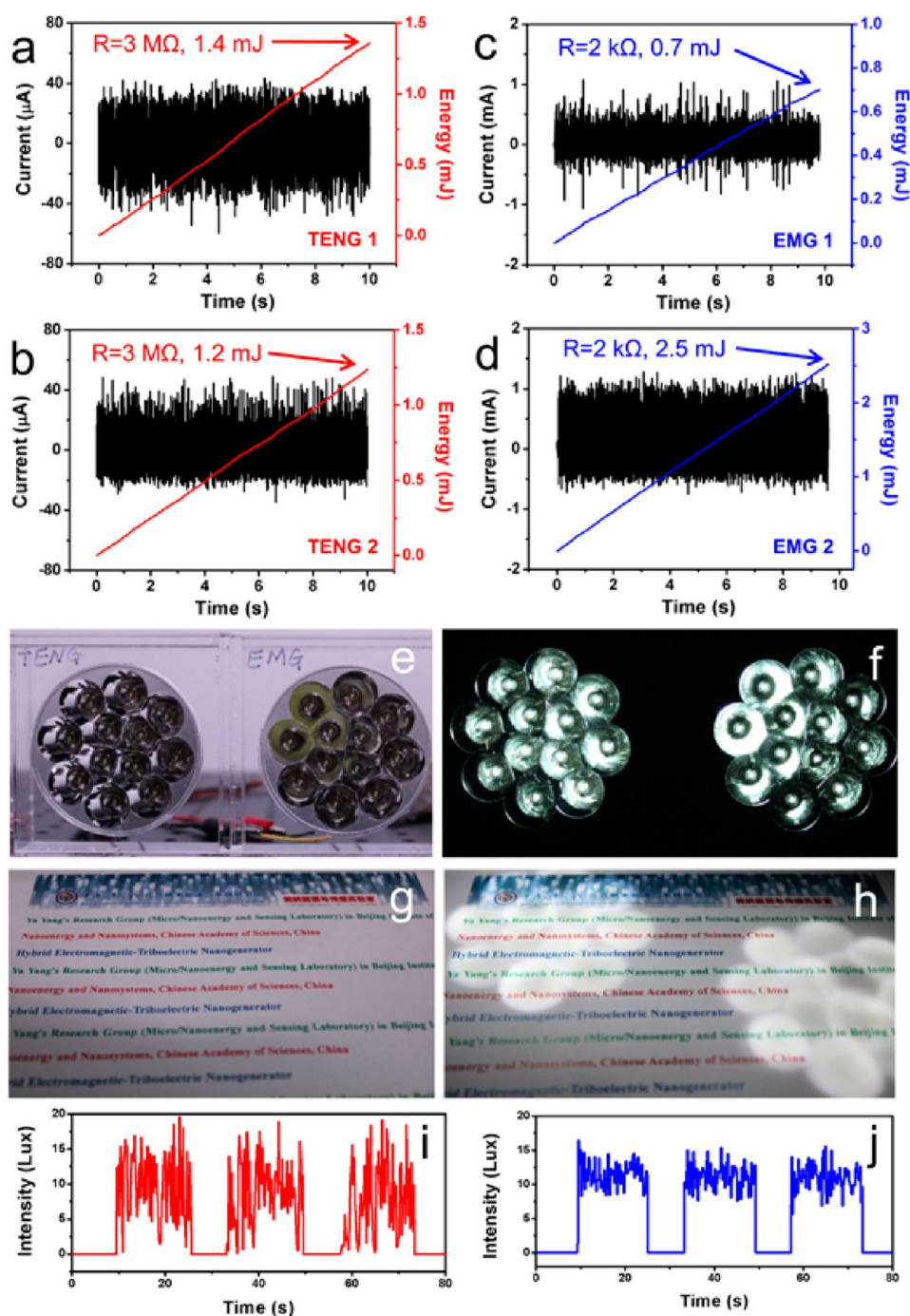
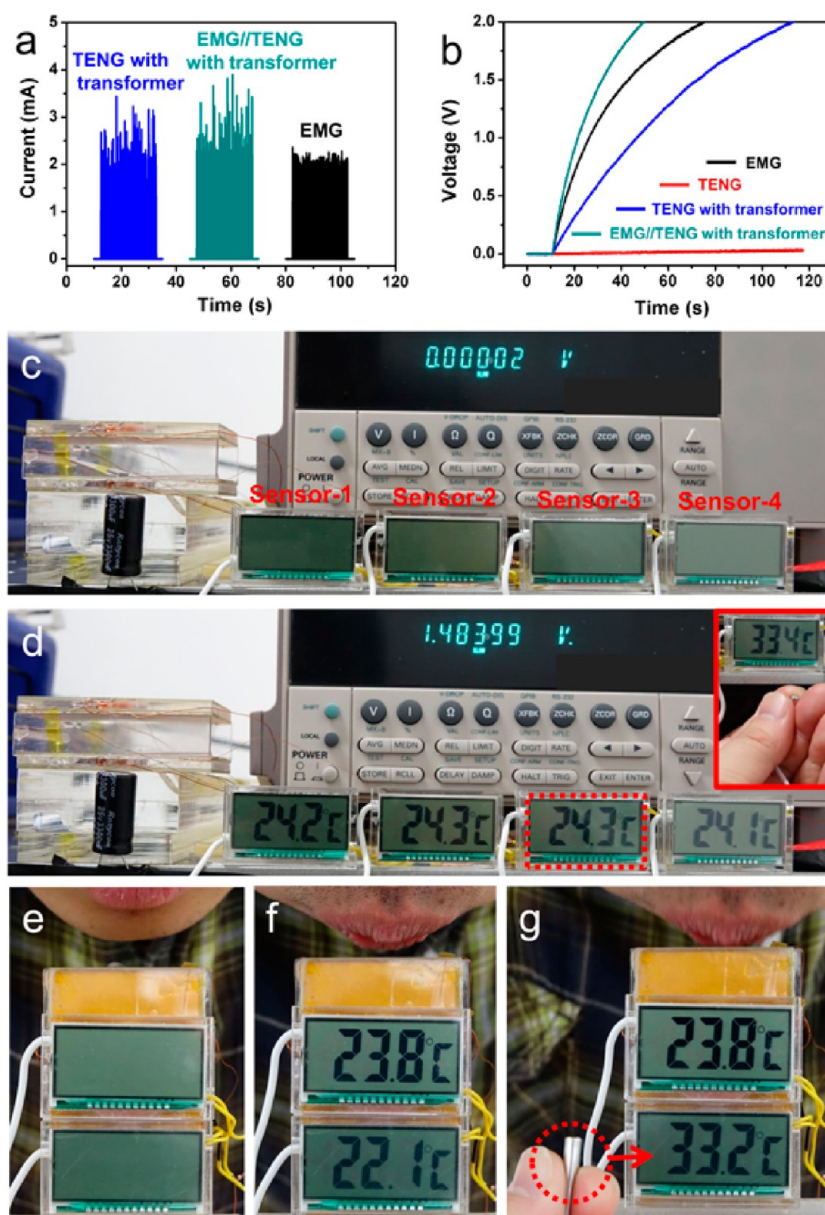


Figure 5. (a, b) Output current and the generated electric energy of TENG 1 (a) and TENG 2 (b) in 10 s. (c, d) Output current and the generated electric energy of EMG 1 (c) and EMG 2 (d) in 10 s. (e) Photograph of two groups of LEDs. (f) Photograph of lighted LEDs by using TENG and EMG. (g) Photograph of a printed text. (h) Photograph of lighted LEDs by the hybridized nanogenerator to provide enough illumination for reading printed text in complete darkness condition. (i, j) Measured illumination intensities of the two groups of LEDs driven by TENG (i) and EMG (j).

observed for the hybridized device as compared with the individual energy harvesting unit, which is associated with the asynchronism for the TENG and EMG.<sup>20</sup> Figure 6b depicts the charging performances of a 3300  $\mu\text{F}$  capacitor by using the different devices, indicating that the hybridized nanogenerator has the best charging performance among these devices, where the charging voltage can be up to 2 V in about 50 s.

Moreover, the charging performance of the capacitor by using the TENG with transformer is much better than that of the TENG without transformer. Figure 6c illustrates a self-powered temperature sensor system, which includes a hybridized nanogenerator, a capacitor of 3300  $\mu\text{F}$ , and four temperature sensors. As displayed in Figure 6d, the four temperature sensors can be sustainably powered when the air-flow driven hybridized



**Figure 6.** (a) Rectified output current signals of the different devices. (b) Measured charging curves of a capacitor with  $3300\ \mu\text{F}$  by using the different devices. (c) Photograph of a self-powered temperature sensor system including a hybridized nanogenerator, a capacitor, and four temperature sensors. (d) Photograph of using the hybridized nanogenerator to sustainably power four temperature sensors, where the inset indicates a increase of temperature by using touching of fingers. (e–f) Photographs of using a hybridized nanogenerator to scavenge human mouth blowing induced air-flow energy to sustainably two temperature sensors.

nanogenerator is working. By finger touching one temperature sensor, the rise of temperature can be recorded in real time, as presented in the inset of Figure 6d (movie file-4, Supporting Information), where the temperature sensor sensing unit is at the end of the white wire. Parts e–g of Figure 6 illustrate that the human mouth blowing induced air-flow energy can be used to power two temperature sensors, where the temperature of the human fingers is about  $33.2\ ^\circ\text{C}$ , as shown in Figure 6g (movie file-5, Supporting Information). Figure S7 (Supporting Information) presents a photograph of the fabricated self-powered temperature sensor system, which includes a hybridized

nanogenerator, a temperature sensor, a capacitor of  $100\ \mu\text{F}$ , and four bridge rectification circuits. The first self-powered temperature sensor system can sustainably work by using a human mouth blowing induced air-flow to drive the hybridized nanogenerator (movie file-6, Supporting Information).

To enhance the output of the hybridized nanogenerators to realize more applications, more rectified devices were integrated in parallel. Figure 7a displays a photograph of four hybridized nanogenerators, which have eight TENGs and eight EMGs. By integrating these units in parallel, the total output current of the hybridized nanogenerators can be up to 5 mA, as presented

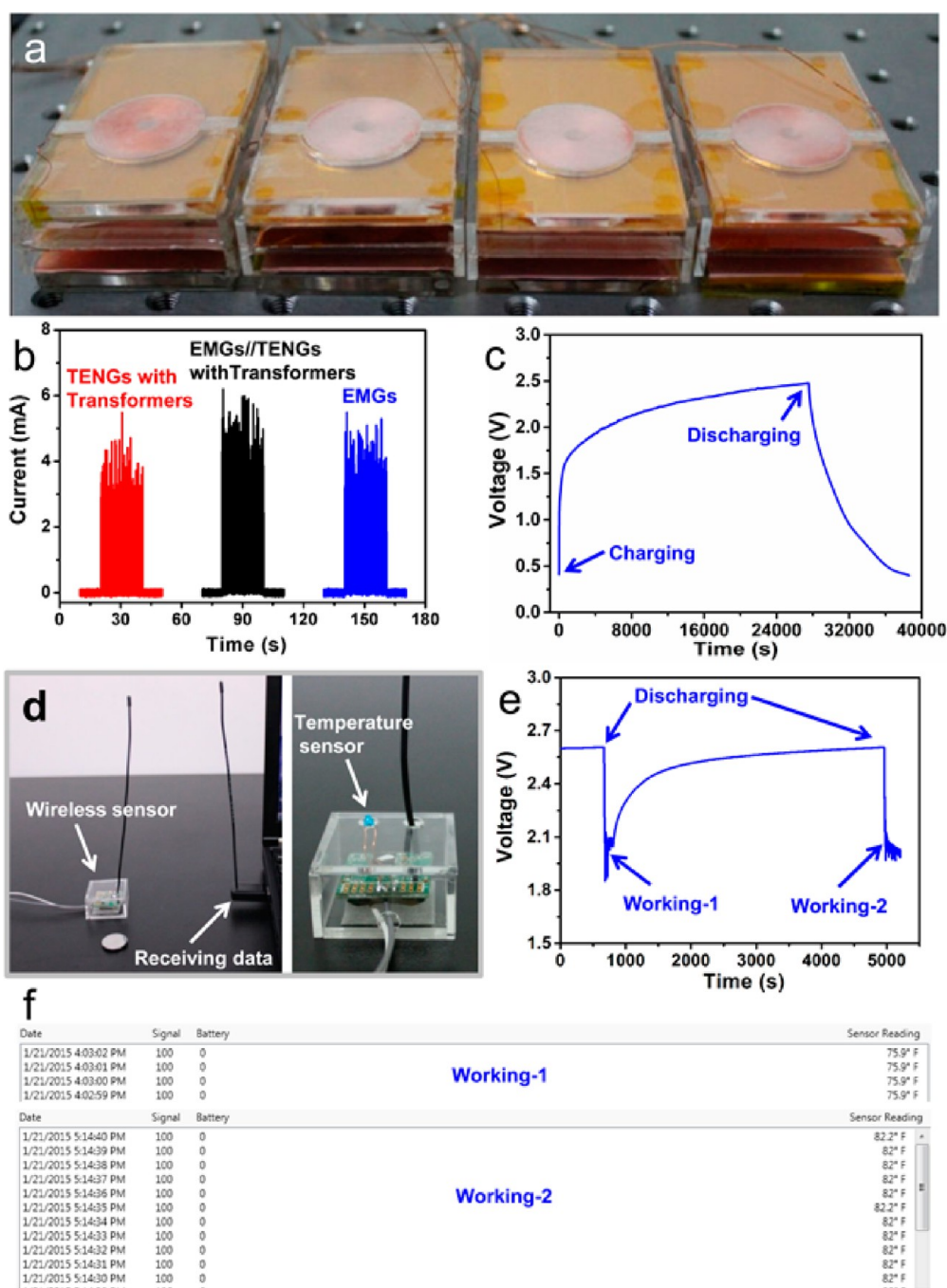


**Figure 7.** (a) Photograph of four hybridized nanogenerators. (b) Rectified output current signals of the different devices. (c) Charging and constant-current discharging curve of a Li-ion battery by using the hybridized nanogenerators. (d) Photograph of a wireless temperature sensor system. (e) Discharging process of the charged Li-ion battery when the wireless temperature sensor is working. (f) Received temperature data by using the charged Li-ion battery in (e).

in Figure 7b. The produced electrical energy can be used to charge a Li-ion battery. As depicted in Figure 7c, the battery can be charged by the hybridized nanogenerators from 0.4 to 2.5 V in about 7.6 h. Under a constant discharging current of 0.1 mA, the time of the voltage drop from 2.5 to 0.4 V is about 3.1 h, resulting in that the stored electric capacity was about 0.31 mAh.

The charged Li-ion battery can be used to sustainably power a wireless temperature sensor. As shown in

Figure 7d, the temperature sensor system includes a wireless temperature sensor and a receiving data device that is connected to a computer, where the temperature data can be observed in the computer. Figure 7e presents the discharging processes of the Li-ion battery when the wireless sensor is working. The received temperature data at a distance of 1.5 m can be seen in Figure 7f, where the temperature is 75.9 K for the status (working-1). We found that the wireless temperature sensor cannot work when the voltage of



the battery is smaller than 2 V, and the battery needs to be charged to 2.5 V, which can drive the wireless sensor to work again. The voltage of the Li-ion battery will be increased due to the charging process of hybridized nanogenerators, which can be seen in Figure 7e (between working-1 and working-2). When the voltage of the battery is larger than 2.5 V, the wireless sensor will work again to send the data to the computer. The received temperature is 82.2 K when the finger was used to touch the temperature sensor. The wireless temperature sensor can sustainably work by using the hybridized nanogenerators charged Li-ion battery.

## CONCLUSIONS

In summary, we have developed the first hybridized electromagnetic–triboelectric nanogenerator for scavenging air-flow energy to sustainably power

temperature sensors. The working principle of the hybridized nanogenerator is based on the air-flow-driven vibration of a kapton film in an acrylic tube to induce the simultaneous working of two TENGs at the free-standing end and two EMGs at the front section. The produced electrical energy of the hybridized nanogenerator is much larger than that generated by an individual energy harvesting unit (TENG or EMG). Under an air-flow speed of 18 m/s, the produced electrical energy can be stored in a capacitor of 3300  $\mu\text{F}$  for sustainably powering four temperature sensors. Moreover, a wireless temperature sensor can be driven by integrating four hybridized nanogenerators to charge a Li-ion battery with the stored electric capacity up to 0.31 mAh. The fabricated hybridized nanogenerators have potential applications for air-flow energy harvesting and self-powered personal electronics/sensors.

## EXPERIMENTAL SECTION

**Fabrication of the Hybridized Nanogenerator.** The fabricated hybridized nanogenerator consists of two TENGs and two EMGs. First, an acrylic tube with the inner dimensions of 6.7 cm  $\times$  4 cm  $\times$  1.2 cm was fabricated by using a laser cutting machine. The two TENGs include a kapton film (50  $\mu\text{m}$ ) with Cu electrodes at the surfaces and two PTFE films (50  $\mu\text{m}$ ) with Cu electrode at one surface. One side of the kapton film was fixed at the middle of the end surface of the acrylic tube, where the other sides are free-standing. The two PTFE films were fixed on the top and bottom inner surfaces of the acrylic tube, respectively. The two TENGs have a total mass of about 0.8 g and the total volume of about  $4.8 \times 10^{-7} \text{ m}^3$ , respectively, where this calculation includes the two PTFE films, one kapton film, and the Cu electrodes. The two EMGs consist of two magnets fixed on the kapton film and two coils fixed on the top and bottom of the acrylic tube. The two EMGs have a total mass of about 12.3 g and a total volume of about  $9.7 \times 10^{-6} \text{ m}^3$ , respectively, where the calculation includes the coils and the magnets. The total mass of the hybridized nanogenerator including the acrylic tube is about 42.3 g and the device has the external dimensions of 6.7 cm  $\times$  4.5 cm  $\times$  2 cm.

**Measurement of the Hybridized Nanogenerator.** In this study, the output electrical signals of the hybridized nanogenerators were obtained by using a low-noise current preamplifier (Stanford Research SR570) and a programmable electrometer (Keithley Model 6514). The dynamic vibration process of the kapton film was captured using a high-speed camera (Phantom, v711) at a frame rate of 7500 Hz.

**Conflict of Interest:** The authors declare no competing financial interest.

**Acknowledgment.** This work was supported by Beijing Natural Science Foundation (2154059), National Natural Science Foundation of China (Grant Nos. 51472055, 61404034, 51432005), Beijing City Committee of science and technology (Nos. Z131100006013004, Z131100006013005), and the “Thousands Talents” program for pioneer researcher and his innovation team, China. One patent has been filed based on the research here.

**Supporting Information Available:** Additional figures including the original data of TENG 1, TENG 2, TENG 1 with transformer, EMG 1, and EMG 2 under different loading resistances. Movie files including the dynamic process for the air-flow driven vibration behavior of the kapton film, the hybridized nanogenerator driven LEDs to provide the illumination for reading

printed text, and the hybridized nanogenerator driven capacitors for sustainably powering temperature sensors. This material is available free of charge via the Internet at <http://pubs.acs.org>.

## REFERENCES AND NOTES

1. Wang, Z. L.; Song, J. Piezoelectric Nanogenerators Based on Zinc Oxide Nanowire Arrays. *Science* **2006**, *312*, 242–246.
2. Sung, J. H.; Heo, H.; Hwang, I.; Lim, M.; Lee, D.; Kang, K.; Choi, H. C.; Park, J.-H.; Jhi, S.-H.; Jo, M.-H. Atomic Layer-by-Layer Thermoelectric Conversion in Topological Insulator Bismuth/Antimony Tellurides. *Nano Lett.* **2014**, *14*, 4030–4035.
3. Zhong, Q.; Zhong, J.; Hu, B.; Hu, Q.; Zhou, J.; Wang, Z. L. A Paper-Based Nanogenerator as a Power Source and Active Sensor. *Energy Environ. Sci.* **2013**, *6*, 1779–1784.
4. Blanco, M. I. The Economics of Wind Energy. *Renew. Sustainable Energy Rev.* **2009**, *13*, 1372–1382.
5. Bilgili, M.; Yasar, A.; Simsek, E. Offshore Wind Power Development in Europe and Its Comparison with Onshore Counterpart. *Renew. Sustainable Energy Rev.* **2011**, *15*, 905–915.
6. Herbert, G. M. J.; Iniyar, S.; Sreevalsan, E.; Rajapandian, S. A Review of Wind Energy Technologies. *Renew. Sustainable Energy Rev.* **2007**, *11*, 1117–1145.
7. Fan, F.-R.; Tian, Z.-Q.; Wang, Z. L. Flexible Triboelectric Generator. *Nano Energy* **2012**, *1*, 328–334.
8. Yang, Y.; Zhou, Y. S.; Zhang, H.; Liu, Y.; Lee, S.; Wang, Z. L. A Single-Electrode Based Triboelectric Nanogenerator as Self-Powered Tracking System. *Adv. Mater.* **2013**, *25*, 6594–6601.
9. Meng, B.; Tang, W.; Too, Z.-H.; Zhang, X.; Han, M.; Liu, W.; Zhang, H. A Transparent Single-Friction-Surface Triboelectric Generator and Self-Powered Touch Sensor. *Energy Environ. Sci.* **2013**, *6*, 3235–3240.
10. Kim, D.; Jeon, S.-B.; Kim, J. Y.; Seol, M.-L.; Kim, S. O.; Choi, Y.-K. High-Performance Nanopattern Triboelectric Generator by Block Copolymer Lithography. *Nano Energy* **2015**, *12*, 331–338.
11. Yang, Y.; Zhu, G.; Zhang, H.; Chen, J.; Zhong, X.; Lin, Z.-H.; Su, Y.; Bai, P.; Wen, X.; Wang, Z. L. Triboelectric Nanogenerator for Harvesting Wind Energy and as Self-Powered Wind Vector Sensor System. *ACS Nano* **2013**, *7*, 9461–9468.
12. Guo, H.; He, X.; Zhong, J.; Zhong, Q.; Leng, Q.; Hu, C.; Chen, J.; Tian, L.; Xi, Y.; Zhou, J. A Nanogenerator for Harvesting Airflow Energy and Light Energy. *J. Mater. Chem. A* **2014**, *2*, 2079–2087.

13. Guo, H.; Chen, J.; Tian, L.; Leng, Q.; Xi, Y.; Hu, C. Airflow-Induced Triboelectric Nanogenerator as a Self-Powered Sensor for Detecting Humidity and Airflow Rate. *ACS Appl. Mater. Interfaces* **2014**, *6*, 17184–17189.
14. Meng, X. S.; Zhu, G.; Wang, Z. L. Robust Thin-Film Generator Based on Segmented Contact-Electrification for Harvesting Wind Energy. *ACS Appl. Mater. Interfaces* **2014**, *6*, 8011–8016.
15. Wang, S.; Mu, X.; Yang, Y.; Sun, C.; Gu, A. Y.; Wang, Z. L. Flow-Driven Triboelectric Generator for Directly Powering a Wireless Sensor Node. *Adv. Mater.* **2015**, *27*, 240–248.
16. Wu, Y.; Wang, X.; Yang, Y.; Wang, Z. L. Hybrid Energy Cell for Harvesting Mechanical Energy from One Motion Using Two Approaches. *Nano Energy* **2015**, *11*, 162–170.
17. Zhang, C.; Tang, W.; Han, C.; Fan, F.; Wang, Z. L. Theoretical Comparison, Equivalent Transformation, and Junction Operations of Electromagnetic Induction Generator and Triboelectric Nanogenerator for Harvesting Mechanical Energy. *Adv. Mater.* **2014**, *26*, 3580–3591.
18. Hu, Y.; Yang, J.; Niu, S.; Wu, W.; Wang, Z. L. Hybridizing Triboelectrification and Electromagnetic Induction Effects for High-Efficient Mechanical Energy Harvesting. *ACS Nano* **2014**, *8*, 7442–7450.
19. Saurenbach, F.; Wollmann, D.; Terris, B. D.; Diaz, A. F. Force Microscopy of Ion Containing Polymer Surfaces: Morphology and Charge Structure. *Langmuir* **1992**, *8*, 1199–1203.
20. Yang, Y.; Zhang, H.; Liu, R.; Wen, X.; Hou, T.-C.; Wang, Z. L. Fully Enclosed Triboelectric Nanogenerators for Applications in Water and Harsh Environments. *Adv. Energy Mater.* **2013**, *3*, 1563–1568.